DEPENDENT COMPONENT ANALYSIS AS A TOOL FOR BLIND SPECTRAL UNMIXING OF REMOTE SENSED IMAGES

C. F. Caiafa [1]*, E. Salerno* [2]*, A. N. Proto* [1,3] *and L. Fiumi* [4]

[1] Laboratorio de Sistemas Complejos. Facultad de Ingeniería. Universidad de Buenos Aires,
Av. Paseo Colón 850. 4to. piso, Ala sur (1063) Capital Federal. Argentina. Email: ccaiafa@fi.uba.ar

[2] Istituto di Scienza e Tecnologie dell'Informazione - CNR
Via Moruzzi, 1, I-56124 Pisa, Italy. Email: emanuele.salerno@isti.cnr.it

[3] Comisión de Investigaciones Científicas de la Prov. de Buenos Aires,
Av. Paseo Colón 850. 4to. piso, Ala sur (1063) Capital Federal. Argentina. Email: aproto@fi.uba.ar

[4] Laboratorio Aereo Ricerche Ambientali. Istituto sull'Inquinamento Atmosferico - CNR,
Via del Fosso del Cavaliere, 100 00133 Roma, Italy. Email: fiumi@pop.iia.cnr.it

ABSTRACT

In this work, we present a blind technique for the estimation of the material abundances per pixel (endmembers) in hyperspectral remote-sensed images. Classical spectral unmixing techniques require the knowledge of the existing materials and their spectra. This is a problem when no prior information is available. Some techniques based on independent component analysis did not prove to be very efficient for the strong dependence among the material abundances always found in real data. We approach the problem of blind endmember separation by applying the MaxNG algorithm, which is capable to separate even strongly dependent signals. We also present a minimum-mean-squared-error method to estimate the unknown scale factors by exploiting the source constraint. The results shown here have been obtained from either synthetic or real data. The synthetic images have been generated by a noisy linear mixture model with real, spatially variable, endmember spectra. The real images have been captured by the MIVIS airborne imaging spectrometer. Our results showed that MaxNG is able to separate the endmembers successfully if a linear mixing model holds true and for low noise and reduced spectral variability conditions.

1. INTRODUCTION

Modern airborne and satellite-borne optical sensors are able to provide a huge amount of data with high resolution in the spatial domain as well as in the spectral domain. Multispectral images, i.e., images with less than ten spectral channels, have allowed whole pixels to be classified [17], but the analysis of the individual substances that constitute each pixel is limited by the small number of channels available [12]. On the other hand, in hyperspectral images, where hundreds of channels are normally available, it is possible to obtain an estimation of the material (endmember) percentages per pixel. This task is called spectral unmixing and is a new and fascinating field of research.

Under certain conditions (see [16], [12] and all the references therein for details), the spectral radiance upon the sensor location can be assumed to be well approximated by a linear mixture of the endmember radiances weighted by the correspondent fractional abundances[1], plus additive noise. This is called the linear mixing model and, basically, it is valid when multiple scattering among distinct endmembers is negligible and the surface is partitioned according to the fractional abundances [12].

Many spectral unmixing algorithms have been developed by exploiting a linear mixing model. The classical approaches require some knowledge of the existing materials and their spectra. If the endmember spectra are known, then the estimation of the abundances is an inverse problem that has been solved, for example, by least squares methods [12] and other approaches [1]. In any case, endmember determination is not an easy task, being usually achieved through an educated trial-and-error approach, and the analyst should have some knowledge of the field. For this reason, during the last years, many efforts were made to derive blind spectral unmixing techniques that may not require users to have any knowledge about the endmembers.

This kind of problem (blind source separation, or BSS) was deeply studied during the last 10 years for the special case where the sources are mutually independent (independent component analysis, or ICA [10], [11]). Some authors applied ICA to the spectral unmixing problem and obtained some promising results [5], [8], [13], [15]. At the same time, however, ICA algorithms did not prove to be well suited for this problem, and many issues are still open to solve. The main reason why ICA is not a good solution is that, in the spectral unmixing framework, the endmember abundances (also referred to as *sources* in the BSS-ICA context) are not independent, being constrained to add up to one [16].

The separation of dependent sources, or dependent component analysis (DCA) [2], [3], was attempted by a few researchers in remote sensing. In [6] and [7], a new algorithm called MaxNG was introduced for the separation of dependent sources, based on a non-Gaussianity measure and using the Euclidean distance between probability distributions calculated by the Parzen windows technique.

In this paper, we propose to approach the spectral unmixing problem through the MaxNG algorithm. This paper is organized as follows: in Section 2, the linear mixing model for

---

[1]The phrase *fractional abundance*, widely used in spectral unmixing papers (see [16]), denotes the percent contribution of an endmember to a pixel.

hyperspectral images is presented, which includes the end-member spectra, their variability and the effects of the system noise; in Section 3, a general presentation of the MaxNG DCA approach is given, along with a useful minimum-mean-squared-error technique for the removal of scale ambiguities; in Section 4, experimental results are presented with synthetic and real data sets; finally, in Section 5, our main conclusions are outlined.

2. HYPERSPECTRAL DATA MODEL

At any fixed pixel, a simplified linear mixing model for M sensors (bands) and P endmembers (usually $P << M$ in hyperspectral images) can be written as follows:

$$\mathbf{x} = \Phi A \mathbf{s} + \mathbf{n} \qquad (1)$$

where $\mathbf{x}$ is a $M \times 1$ vector which contains random variables assigned to the measures for each band, A is the mixing matrix $(M \times P)$, which contains the spectral signatures of the endmembers $\mathbf{s}$ existing in the covered area, Φ is a diagonal random matrix with $E[\Phi] = I$ (where $E[\cdot]$ means expectation) that represents the spatial variability of the endmember spectra, and $\mathbf{n}$ is a $M \times 1$ vector containing the system noise. Note that effects that are often important, such as the ones derived from the topography, are not included in this simple model.

3. DEPENDENT COMPONENT ANALYSIS APPROACH

For simplicity, we restrict the analysis of the linear mixing model in Equation (1) to the noiseless case. We consider the following model, which is expected to be very close to reality in low-noise cases:

$$\mathbf{x} = A\mathbf{s} \qquad (2)$$

If A is known, then the solution can be obtained by using the pseudoinverse matrix, i.e. $\mathbf{s} = A^\dagger \mathbf{x}$ $(A^\dagger = (A^T A)^{-1} A^T)$.

Some preprocessing steps are needed in order to enable MaxNG to work correctly. As it is also usual in ICA, we first need to remove the mean data vector and to apply a spatial whitening filter. This is to obtain uncorrelated unit-variance variables and, at the same time, to reduce the dimensionality of the data[2]. It is important to stress that the purpose of spatial whitening is also to restrict the solution to unit-variance source estimates (see [7] for details). To this purpose, we define the centered vectors $\mathbf{s}' = \mathbf{s} - \overline{\mathbf{s}}$ and $\mathbf{x}' = \mathbf{x} - \overline{\mathbf{x}}$ (where $\overline{\mathbf{s}} = E[\mathbf{s}]$ and $\overline{\mathbf{x}} = E[\mathbf{x}]$). To reduce the dimensionality of the data and decorrelate them, we use the classical principal component analysis [11], i.e. we define the following Q-vector:

$$\widetilde{\mathbf{x}} = \Lambda^{-1/2} V^T \mathbf{x}' \qquad (3)$$

where V is the $M \times Q$ $(Q \leq P < M)$ matrix of the Q dominant eigenvectors of the covariance matrix $R_{\mathbf{x}'\mathbf{x}'} = E[\mathbf{x}'\mathbf{x}'^T]$ and Λ is the diagonal matrix of the related eigenvalues[3].

In the blind scenario, A is unknown and our DCA algorithm should estimate the sources $\widehat{\mathbf{s}}$ by finding a separation matrix $\widetilde{D}$ that verifies the following relationship:

---

[2]For example, one of our data sets has $M = 102$ mixtures (sensors), and the expected number of sources is 9. This makes the data set highly redundant.

[3]Note that, if no noise is considered in the model, the actual dimensionality of the data space is $Q = P - 1$, because the sources are restricted to add up to one, thus reducing by one the effective dimensions.

$$\widehat{\mathbf{s}} = W\mathbf{s}' = \widetilde{D}\widetilde{\mathbf{x}} \qquad (4)$$

where W is a permutation and/or scale matrix [9], [11].

The MaxNG algorithm searches for the matrix $\widetilde{D}$ row by row, by maximizing a measure of non-Gaussianity and restricting the search over the unit-variance source subspace (see [7] and [6] for details). It is important to bear in mind that maximizing non-Gaussianity is equivalent to minimizing mutual information only for independent sources, which is not the case in hyperspectral images.

3.1 Scale ambiguity treatment

Like most BSS algorithms, and as is apparent in Equation (4), MaxNG provides an estimate of the sources up to scaling and permutation. The permutation indeterminacy is not important for our purposes, but scaling is critical for allowing us to make a correct interpretation of the results, taking into account that, in general, different scale factors can be observed for different sources. Assuming no permutation, we formally define the vector of scale factors as follows: $\mathbf{h}^T = [h_0 \quad h_1 ..... h_{P-1}]$. For each centered source, we have $s_i' = h_i \widehat{s}_i$.

Our idea to solve the scale ambiguity is to use the constraint on sources $(\sum_{i=0}^{P-1} s_i = 1)$ for the calculation of the scale factor vector $\mathbf{h}$. First, we note that, for the centered sources, the above constraint implies $\sum_{i=0}^{P-1} s_i' = 0$. In a real-world situation, this summation will not be exactly equal to zero but it may be small enough. Therefore, we define the mean square error as follows: $\rho = E\left[\left(\sum_{i=0}^{P-1} s_i' - 0\right)^2\right]$. Working with this expression and setting it to zero (the minimum attainable error), we finally obtain the following result:

$$\rho = \sum_{i=0}^{P-1} \sum_{j=0}^{P-1} h_i h_j E[\widehat{s}_i \widehat{s}_j] = \mathbf{h}^T R_{\widehat{\mathbf{s}}\widehat{\mathbf{s}}} \mathbf{h} = 0 \qquad (5)$$

Looking at Equation (5), we conclude that any scale factor vector $\mathbf{h}$ that lets the mean squared error be zero belongs to the null space of the covariance matrix $R_{\widehat{\mathbf{s}}\widehat{\mathbf{s}}}$. Note that the constraint on sources implies that the dimensionality of the source space is reduced by one and, therefore, the existence of a non-empty null space is guaranteed.

3.2 Further indeterminacy calculation

From the result obtained in the previous subsection, we observe that the scale factor vector $\mathbf{h}$ cen be determined up to a global scale factor α, which remains undetermined. However, we observe that the determination of vector $\mathbf{h}$ is the most important step, and no further indeterminacy analysis is needed because knowledge of $\mathbf{h}$ allows the analyst to compare the estimated fractional abundances in the same scale.

For a further indeterminacy analysis, and assuming no permutation ambiguity, we have that abundance estimates are:

$$\mathbf{s} = \overline{\mathbf{s}} + \alpha \Theta \mathbf{s}' \qquad (6)$$

where Θ is a $P \times P$ diagonal matrix with $h_0, h_1, ..., h_{P-1}$ as elements of the main diagonal.

For a complete determination of the source estimates, we still need to calculate $P + 1$ parameters: $\overline{s}_0, \overline{s}_1, ..., \overline{s}_{P-1}$ and

α.[4] It is important to note that, if the mixing matrix A is known, using Equations (2) and (4), we can calculate all the missing parameters using the following formulae:

$$\bar{\mathbf{s}} = A^\dagger \bar{\mathbf{x}} \qquad (7)$$

$$\alpha h_i = \sqrt{[A^\dagger R_{\mathbf{x}'\mathbf{x}'} A^{\dagger T}]_{(i,i)}} \qquad (8)$$

where the notation $[\cdot]_{(i,i)}$ stands for the element of row i and column i of the matrix in brackets.

Of course, in a blind scenario, we don't have access to A and we should estimate the parameters $\bar{\mathbf{s}}$ and α by using some assumption on the available dataset. For example, if we assume that there are some pixels where an endmember has zero abundance, and some other pixels with only one endmember, then we can adjust the parameters by forcing some abundances to the values zero or one in the selected pixels.

4. EXPERIMENTAL RESULTS

In this section, we present some experimental results that show the efficiency of MaxNG as a tool for blind spectral unmixing of hyperspectral images. In order to evaluate the proposed separations, we need to know exactly which are the original material abundances. To this purpose, in the first part of our experiments, we present the results obtained by applying MaxNG to a synthetic dataset and compare our source estimates with the original sources. We evaluate the performance of the algorithm for the cases of additive noise and of random spectral variability. In the second part of our experiments, we apply MaxNG directly to a real hyperspectral image.

For our experiments, we used a real, radiometrically corrected hyperspectral image of a Rome city area, and a ground truth classification in nine classes, both provided by the Airborne Laboratory for Environmental Research at IIA-CNR in Rome, Italy (see Fig. 1). The 540×337-pixel original image comes from the MIVIS sweepbroom airborne imaging spectrometer, and contains 102 spectral channels from four independent sensors in different bands: channels $1 - 20$ ($0.43 - 0.83\mu m$); channels $21 - 28$ ($1.15 - 1.55\mu m$); channels $29 - 92$ ($2.00 - 2.50\mu m$) and $93 - 102$ ($8.20 - 12.70\mu m$). The classification map (Fig. 1, bottom) has been obtained by the standard spectral angle mapper (SAM) method [14] integrated by a series of color stereo images and direct field inspections. The classes extracted are: bricks (red), grit (yellow), other surfaces (grey), infrastructures (brown), trees (dark green), bush (green), meadows (light green), water (blue) and unclassified (black).

4.1 Synthetic data

A synthetic data set was simulated using real spectra. For the calculation of each endmember spectrum, we took the average of the spectra of pixels belonging to each class.[5] Using the original classification image (Fig. 1, bottom) we generated a simulated low resolution image by mixing the spectra of existing materials for each 8×8 pixel subarea. In this way,

---

[4]Actually, only P parameters are missing because, having $P - 1$ entries of $\bar{\mathbf{s}}$, we can derive the missing entry by using the source constraint.

[5]It is obvious that each pixel is not composed by only one material, but this is not important for the purpose of this test.
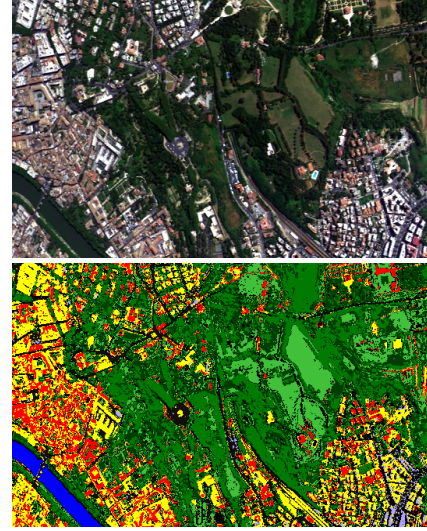

Figure 1: Top: RGB channels of our original hyperspectral image (540×337 pixels). Bottom: ground truth image; nine classes are provided.
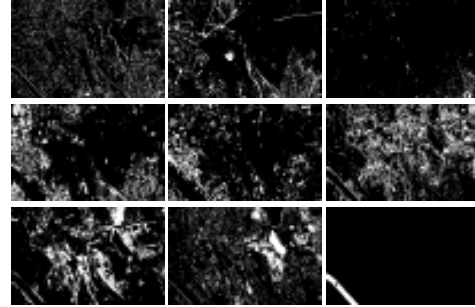

Figure 2: Images corresponding to material abundances (nine endmembers). Zero corresponds to black and one corresponds to white.

we were able to calculate the material abundances as the percentages of the classes contained in each subarea. In Fig. 2, the nine material abundances are shown.

In order to quantify estimation accuracy, we used a measure of closeness of source estimates to the original sources. For each pixel, we define the error vector as the difference between the estimated and the original source vectors, $\mathbf{e} = \mathbf{s}_{estimated} - \mathbf{s}$. On this basis, we evaluate the signal-to-interference ratio (SIR) as it is usually adopted in the literature, that is, for the i-th source: $SIR_i = 10\log_{10}(var(s_i)/var(e_i))$. In general, SIR values below a 10-12 dB threshold are indicative of a failure in obtaining the desired source separation [4].

As a first experiment, we applied MaxNG to hyperspectral data generated with Equation (1) in an ideal scenario with no noise ($\mathbf{n} = \mathbf{0}$) and no spectral variability ($\Phi = I$). In Table 1, the SIR values obtained for each source are shown. Note that all the sources were perfectly recovered from their mixtures.
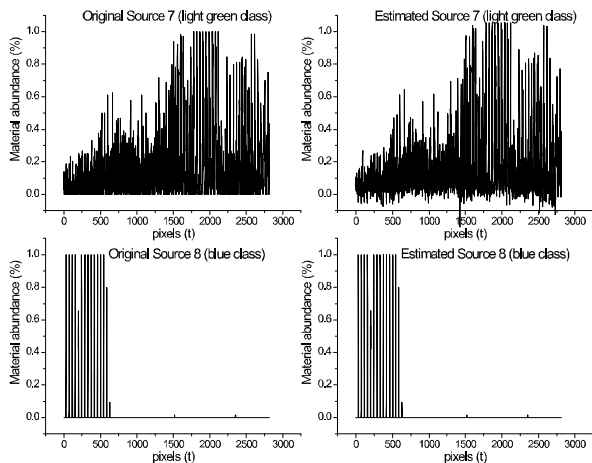
Figure 3: Comparison of original and estimated sources for the light green class (source 7, top) and the blue class (source 8, bottom)

End member	SIR (dB)
0	22.5
1	17.9
2	35.7
3	15.0
4	26.9
5	18.4
6	20.3
7	14.6
8	63.8
Mean SIR	**26.1**

Table 1: SIR values of abundance estimates (no noise and no spectral variability)

For a visual comparison of the results, in Fig. 3, two original sources (meadows - light green, and water - blue) and their estimates are shown as time series. These are the classes estimated with minimum and maximum SIR, respectively (see Table 1). To normalize the source estimates, Equations (7) and (8) were used.

The second experiment consisted in applying MaxNG to a data set generated by using Equation (1) again, with $\Phi = I$ and with different levels of Gaussian noise $\mathbf{n}$. For each channel, we define the Signal To Noise Ratio (SNR) as usual by $SNR(dB) = 20\log\left(\frac{\sigma_x}{\sigma_n}\right)$, where σ_x is the standard deviation of the useful signal in the channel and σ_n is the standard deviation of noise added to the channel. The results are shown in Fig. 4, left panel.

As a third experiment, the spectral variability was simulated and the data were generated again through Equation (1) with $\mathbf{n} = \mathbf{0}$ and matrix Φ composed by random variables with unit mean and different standard deviations. The results are shown in Fig. 4, right panel.

4.2 Real Data

As a final experiment, we applied MaxNG to a portion of the original image. A small piece of 50×50 pixels was selected to minimize the spectral variability and the topographic ef-
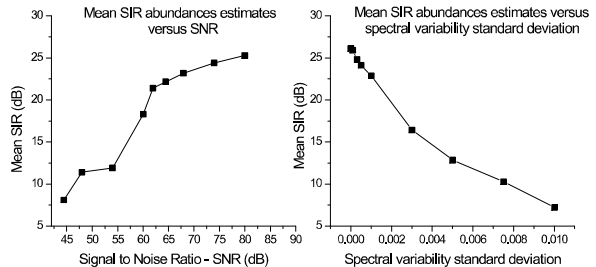

Figure 4: Mean SIR value obtained as a function of the noise level (left) and as a function of the spectral variability (right).
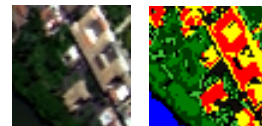

Figure 5: Hyperspectral image (50×50) under analysis in RGB format (left) and its ground-truth image (right).

fects. In Fig. 5, we show the selected area and the related ground truth.

MaxNG has detected six materials, but it is important to note that some of the sources detected are possibly false local maxima of the nongaussianity measure, and must be discarded. After a visual analysis of the sources detected, it seems that only four sources correspond to actual materials. The scale ambiguity removal technique was applied in order to reach a set of comparable material abundances. In Fig. 6, the four materials detected are shown. By visual inspection, it is easy to identify the detected sources: source a) corresponds to grit (yellow), source b) to brick (red), source c) to trees, bush and meadows (green) and source d) to water (blue).

5. CONCLUSIONS

A new approach to blind spectral unmixing was proposed, based on a recently presented DCA algorithm called MaxNG [7], [6]. This approach avoids the problem existing in ICA because the independence of sources is not required. We have presented a set of experimental results showing that
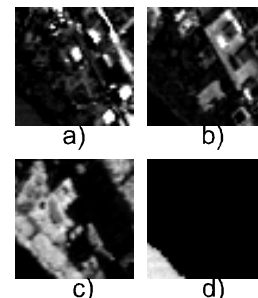

Figure 6: Detected material abundances

MaxNG is able to separate material abundances from synthetic hyperspectral images generated by using real spectra. The effects of additive noise and spectral variability were also analyzed. The problem of scale ambiguity in ICA/DCA was approached and a solution was proposed. Exploiting the source constraint, we have obtained a way of calculating the scale factors in a blind fashion, which is really important because it allows the analyst to make comparisons among detected sources with the same scale and sign.

Finally, a real image example was presented, showing that real material abundances seem to be correctly separated by using MaxNG. As an open issue of this approach, we should mention that MaxNG can detect more sources than actual materials present in the scene, because false local maxima can be present in the optimization landscape [7], [6]. The user needs to visually evaluate all the sources detected to decide which of them are acceptable and which are not.

As a final remark, we say that additive noise and spectral variability noticeably affect the estimation, but the results obtained on real data show that the algorithm is able to separate endmembers with results that are comparable with the ones available in the literature (for example in [16]).

6. ACKNOWLEDGEMENTS

REFERENCES

[1] J. B. Adams, and M. O. Smith, "Spectral mixture modelling: A new analysis of rock and soil types at the Viking Lander 1 Site", *Journal of Geophysical Research*, Vol 91, pp. 8098-8112, 1986.

[2] A. K. Barros, "The independence assumption: dependent component analysis", in M. Girolami (Ed.), *Advances in Independent Component Analysis* (pp. 63-71), Springer-Verlag, London 2000.

[3] L. Bedini, D. Herranz, E. Salerno, C. Baccigalupi, E. Kuruoglu, A. Tonazzini, "Separation of correlated astrophysical sources using multiple-lag data covariance matrices", *Eurasip J. on Appl. Sig. Proc*., Vol. 2005, No. 15, pp. 2400-2412, 21 August 2005.

[4] R. Boscolo, H. Pan and V. P. Roychowdhury, "Independent Component Analysis Based on Nonparametric Density Estimation", *IEEE Trans. on Neural Networks*, Vol. 15, pp 55-65, 2004.

[5] A. Bijaoui, D. Nuzillard and T. Deb Barma, "BSS, Classification and Pixel Demixing", in *Proc. 5th International Conference on Independent Component Analysis and Blind Source Separation* (pp. 96-103), University of Granada (Spain), 2004.

[6] C. F. Caiafa and A. N. Proto, "A non-Gaussianity measure for blind source separation", *in Proc. of SPARS05*, Nov. 16-18, 2005 – IRISA - Rennes (France).

[7] C. F. Caiafa and A. N. Proto, "Separation of statistically dependent sources using an L^2-distance non-Gaussianity measure ", *Signal Processing*, (in press) (Available online 24 March 2006).

[8] Shao-Shan Chiang Chein-I Chang Irving W. Ginsberg, "Unsupervised Hyperspectral Image Analysis Using Independent Component Analysis", in *Proc. IGARSS 2000* (pp. 3136 - 3138), Honolulu Hawaii, July 24-28, 2000.

[9] P. Comon, "Independent Component Analysis, a new concept?", *Signal Processing*, Vol 36, pp. 287-314, 1994.

[10] A. Cichocki and S. Amari. *Adaptive Blind Signal and Image Processing: Learning Algorithms and Applications*. J. Wiley & Sons, Chichester UK, 2002.

[11] A. Hyvärinen, J. Karhunen and E. Oja, *Independent Component Analysis*, J. Wiley & Sons, New York, 2001.

[12] N. Keshava and J. Mustard, "Spectral unmixing", I*EEE Signal Process. Mag*., Vol. 19, no. 1, pp. 44–57, 2002.

[13] Naoko Kosaka, Kuniaki Uto, and Yukio Kosugi, "ICA-Aided Mixed-Pixel Analysis of Hyperspectral Data in Agricultural Land", *Geoscience and Remote Sensing Letters, IEEE*, Vol 2, pp.220 - 224, April 2005

[14] Kruse, F., Lefkoff, A., Boardman, J., Heidebrecht, K., Shapiro, A., Barloon, P. & Goetz, A. "The spectral image processing system (SIPS) - interactive visualization and analysis of imaging spectrometer data". *Remote Sensing of Environment*, Vol. 44, pp. 145-163, 1993.

[15] M. Lennon, G. Mercier, M.C. Mouchot, L. Hubert-Moy "Spectral unmixing of hyperspectral images with the Independent Component Analysis and wavelet packets", in *Proc. of the International Geoscience and Remote Sensing Symposium* (pp. 2887-2889), Sydney, Australia, July 9-13, IEEE, 2001.

[16] J. M. P. Nascimento, and J. M. Bioucas Dias. "Does Independent Component Analysis Play a Role in Unmixing Hyperspectral Data?". *IEEE Transactions on Geoscience and Remote Sensing*, Vol. 43, pp. 175-187, January 2005.

[17] B. Tso and P. M. Mather, "Classification methods for remotely sensed data", Taylor and Francis Inc, New York, 2001.